

## Performance Enhancement of Poly (Vinyl Alcohol) Composite Polymer Electrolyte for Li-Ion Battery Through Salt Immersion Process

Christin Rina Ratri\*, Qolby Sabrina, Titik Lestariningsih and Salsabila Zakiyyah

Research Centre for Advanced Materials, National Research and  
Innovation Agency (BRIN),  
Kawasan Puspiptek Gd. 440–441, Tangerang Selatan, 15314 Indonesia

\*Corresponding Author: [christin.rina.ratri@brin.go.id](mailto:christin.rina.ratri@brin.go.id)

Published online: 30 November 2022

To cite this article: Ratri, C. R. et al. (2022). Performance enhancement of poly (vinyl alcohol) composite polymer electrolyte for li-ion battery through salt immersion process. *J. Phys. Sci.*, 33(3), 33–44. <https://doi.org/10.21315/jps2022.33.3.2>

To link to this article: <https://doi.org/10.21315/jps2022.33.3.2>

**ABSTRACT:** *Poly (vinyl alcohol) (PVA) composite membrane as separator-cum-electrolyte for li-ion battery was prepared via solution casting method. Hydrophilicity of PVA helped to substitute flammable, toxic solvents with deionised water. Lithium bis(oxalato) borate (LiBOB) electrolyte salt was incorporated in the membrane to form flexible self-standing membrane of composite polymer electrolyte (CPE). To further enhance the ionic conductivity, CPE membrane was immersed in 1M LiBOB salt dissolved in deionised water. Neat PVA membrane would have been dissolved instantly in any solution involving water; introduction of LiBOB electrolyte salt deprived the hydrogen bond which transform it into an insoluble CPE membrane. EIS measurement showed that salt immersion boosted the CPE membrane ionic conductivity by four orders of magnitude, from  $4.77 \times 10^{-7}$  S/cm to  $1.93 \times 10^{-3}$  S/cm at room temperature.*

**Keywords:** LiBOB, polymer composites, polymer membranes, Li-ion battery, salt immersion

### 1. INTRODUCTION

The rise of renewable energy starts to demand the advancement of energy storage. The development of lithium-ion (Li-ion) battery is also pushed constantly beyond the limit, answering challenge proffered by rapid progress of modern gadgets and sophisticated electronic devices.<sup>1</sup>

As a crucial element of Li-ion batteries, electrolyte materials and performance were observed from many points of view. Commercially available Li-ion battery containing liquid electrolyte possess high conductivity, but its long-term stability is hindered by possible leakage and solvent evaporation.<sup>2,3</sup> Furthermore, recent events have shown that even these modern batteries are inevitably prone to fire and explosion.<sup>4</sup> Substantially, these problems can be easily answered by polymer electrolytes if not for their relatively low conductivity at ambient temperature.<sup>5,6</sup> Polymer electrolyte membrane also shows poor behaviour when in contact with electrodes. Advanced polymer electrolyte composites incorporate plasticisers as well as ceramic and oxide fillers to decrease polymer crystallinity, therefore enhancing its ionic conductivity.<sup>7</sup>

Lithium bis(oxalato)borate,  $\text{LiBC}_4\text{O}_8$  (LiBOB) was proposed as potential substitute for conventional lithium hexafluorophosphate ( $\text{LiPF}_6$ ) electrolyte salt. LiBOB offers better thermal stability as high as  $300^\circ\text{C}$  and is proven to increase the amorphousness of polymer electrolyte complex.<sup>8</sup> Unlike  $\text{LiPF}_6$ , LiBOB does not release harmful gases upon contact with the slightest amount of moisture owing to its fluorine-free structure.<sup>9</sup> Polyethylene oxide (PEO) was opening the path of polymer electrolyte research, but its poor mechanical integrity still needs more improvement.<sup>10</sup> Poly (vinyl alcohol) (PVA) was used instead in this study due to its non-toxic trait as well as its mechanical and electrical properties.<sup>11</sup> Excellent solubility of PVA in water helps further in eliminating the use of N, N-Dimethylacetamide (DMAc) solvent, which was identified by the European Commission of Health Agency as a substance of a very high concern (SVHC) due to having the status of medium potency reproductive toxicant.<sup>12</sup>

This study reports fabrication and characterisation of PVA/LiBOB composite polymer electrolyte. The resulting membrane was immersed in electrolyte solution containing LiBOB salt. Typically, electrolyte salt is dissolved in carbonate solvent before assembling into battery cell. In this experiment LiBOB was dissolved in deionised water. In the relevant studies thus far, we have found several examples of solid polymer electrolyte immersed in carbonate-based liquid electrolyte as well as basic solution, but no mention of aqueous electrolyte salt solution.<sup>13–16</sup>

## 2. EXPERIMENTAL METHOD

### 2.1 Fabrication of Solid Polymer Electrolyte

PVA (MW 31,000–50,000, 87–89% hydrolysed, Aldrich) was used without further treatment. LiBOB (Aldrich) was heated overnight to remove trace moisture. Deionised water was obtained from Evoqua LaboStar PRO TWF UV ultra-pure water system with measured conductivity at  $0.055\ \mu\text{S}$ .

PVA-based composite polymer electrolyte was prepared by solution casting method. The composition of PVA and deionised water was kept at 1:10 w/v. PVA solution was stirred vigorously for 3 h–4 h at 90°C until all solute dissolves into clear solution. LiBOB electrolyte salt of 20% PVA weight was subsequently added. It was stirred for two more hours until homogeneous, opaque slurry was obtained.

The solution was then cast onto a petri dish, where it was placed in a desiccator at room temperature for 72 h. Free-standing film of polymer electrolyte membrane, denoted by sample PVA-20, was peeled from petri dish, and stored in a dry box to prevent moisture contamination. Similar membrane was fabricated only with PVA without salt electrolyte, denoted as sample PVA-0.

## 2.2 Membrane Immersion

Swelling behaviour was observed prior to membrane immersion. The 1M LiBOB liquid electrolyte was prepared by dissolving appropriate amount of LiBOB salt in deionised water. PVA membranes obtained from previous step was cut into a circle with 17 mm diameter and then immersed into the solution for a certain amount of time until it reached equilibrium. The electrolyte uptake,  $E$ , of PVA-LiBOB membranes was measured using following equation:

$$E = \frac{W_t - W_0}{W_0} \times 100\% \quad (1)$$

where  $W_t$  and  $W_0$  are the weight of the wet and dry membrane, respectively. For wet membrane weight measurement, the membrane was taken off the solution and the surface were wiped gently using filter paper. After final measurement, the membrane (denoted as PVA-20-IM) was dried in the oven to fully evaporate the remaining solvent.

## 2.3 Material Characterisation

The ionic conductivity of the composite polymer electrolyte (CPE) membrane was determined using electrochemical impedance spectroscopy (EIS). The CPE sandwiched between two stainless steel (SS) blocking electrode resulting in SS/CPE/SS configuration in the CR2032 coin cell as shown on Figure 1. EIS measurements were conducted using Metrohm Autolab Nova in the frequency range of 0.1 Hz–50 kHz.

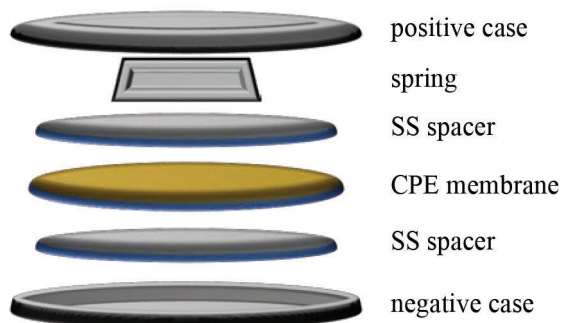


Figure 1: Schematic diagram of CR2032 coin cell configuration for EIS measurement.

Functional groups and their interaction within the polymer electrolyte membranes were observed using FTIR spectroscopy ThermoScientific Nicolet iS10, working at wavenumber range of  $4,000\text{ cm}^{-1}$ – $400\text{ cm}^{-1}$ . X-ray diffraction spectra of the composite polymer membranes were performed using Rigaku Smartlab with  $\text{CuK}\alpha$ , working at  $2\theta$  value range of  $10^\circ$ – $90^\circ$ . Lithium concentration within solution before and after salt immersion was measured using ICP-OES Agilent Technologie.

Surface and cross section morphology were investigated by scanning electron microscope (SEM) Hitachi SU-3500 operated at 5 kV to minimise beam damage. All samples were gold-coated using ion sputtering prior to observation.

### 3. RESULTS AND DISCUSSION

Surface and cross-section morphology of PVA membrane without electrolyte salt addition was shown on Figure 2(a). It displays smooth and homogeneous surface across the surface and cross-section. Membrane thickness of  $100\text{ }\mu\text{m}$  (inset) was measured with the help of ImageJ software. Shards of LiBOB particle on smooth PVA matrix was displayed on Figure 2(b), indicating homogeneous mixing of the CPE precursor. The polymer substrate appeared as smooth as neat PVA film. Membrane thickness (inset) was increasing to  $148\text{ }\mu\text{m}$  with homogeneous layer across the cross section, top to bottom.

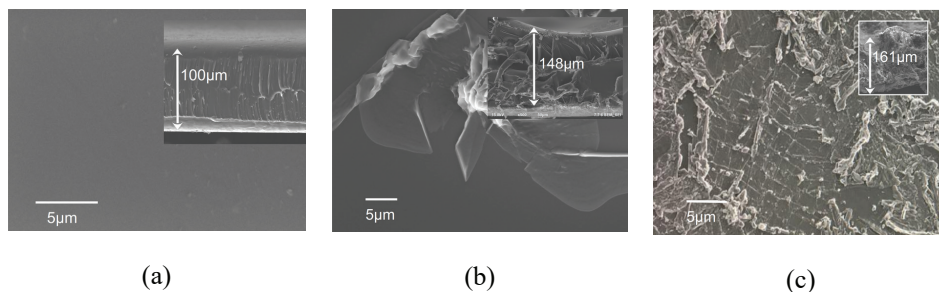


Figure 2: SEM micrographs of (a) PVA film, (b) PVA-20 and (c) PVA-20-IM.

After immersion, however, salt particles were seen spreading atop the substrate, giving rough appearance (Figure 2[c]). Small pores shown in the inset of Figure 2(c) are also visible, giving way to Li atoms to move between electrodes.

Shown on Figure 3 are FTIR spectra for pure PVA and LiBOB in powder state, and the dried CPE membranes. Neat PVA on Figure 3(a) was characterised by peak absorptions located at  $3,307\text{ cm}^{-1}$ ,  $2,916\text{ cm}^{-1}$  and  $1,100\text{ cm}^{-1}$  which corresponds to  $\text{—OH}$ ,  $\text{C—H}$ , and  $\text{C—C—O}$  vibration, respectively.<sup>17</sup>  $\text{C—O}$  stretching was indicated at  $1,095\text{ cm}^{-1}$ .<sup>18</sup> These peaks were strikingly similar to PVA-0 spectra, which suggested mixing, casting and drying process have no influence on the functional groups.

Characteristic peaks of LiBOB material were shown on Figure 3(c), such as  $1,820\text{ cm}^{-1}$  for  $\text{C=O}$  stretching and  $1,415\text{ cm}^{-1}$  for  $\text{C—C=O}$  stretching, then  $1,307\text{ cm}^{-1}$ ,  $1,205\text{ cm}^{-1}$  and  $1,087\text{ cm}^{-1}$  for vibration of  $\text{CO—B—OC}$ ,  $\text{O—C=O}$  and  $\text{O—B—O}$ , respectively. Peaks around  $1,630\text{ cm}^{-1}$  corresponds to  $\text{O—H}$  stretching and bending of adsorbed water.  $\text{O—H}$  bending of crystal water was indicated on peaks around  $1,670\text{ cm}^{-1}$ – $1,685\text{ cm}^{-1}$ . Crystal water was formed upon prolonged exposure of LiBOB powder (or membranes) in highly humid atmosphere.<sup>9</sup>

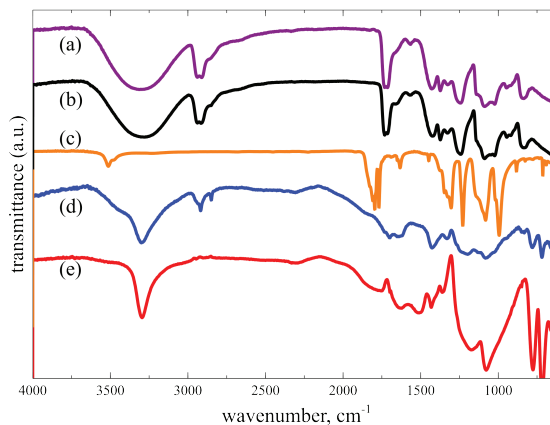


Figure 3: FTIR spectra of (a) PVA powder, (b) PVA-0, (c) LiBOB powder, (d) PVA-20 and (e) PVA-20-IM.

After immersion process, C-H vibration around wavenumber  $2,907\text{ cm}^{-1}$  has diminished into almost unseen peak, indicating LiBOB salt aggregation due to the final drying process. This was also confirmed by the SEM observation seen on Figure 2(c). Peak shifting as well as new peaks, however, arises because of increasing polymer-Li interaction. Shifting of C-O peak around  $1,095\text{ cm}^{-1}$  indicates coordination between Li cations from LiBOB and the PVA substrate. Immersion process apparently also helps with LiBOB complexation in the substrate, seen from LiBOB fingerprints on Figure 3(d) has disappeared or shifted on Figure 3(e).

X-ray diffraction patterns of pure PVA and LiBOB powder as well as CPE membranes were shown on Figure 4. The d-values for pure LiBOB salts have been found to match with ICDD data.<sup>19</sup> Prominent peak around  $2\theta = 19^\circ$  indicates semi-crystalline nature of pure PVA both in powder and membrane form.<sup>20</sup>

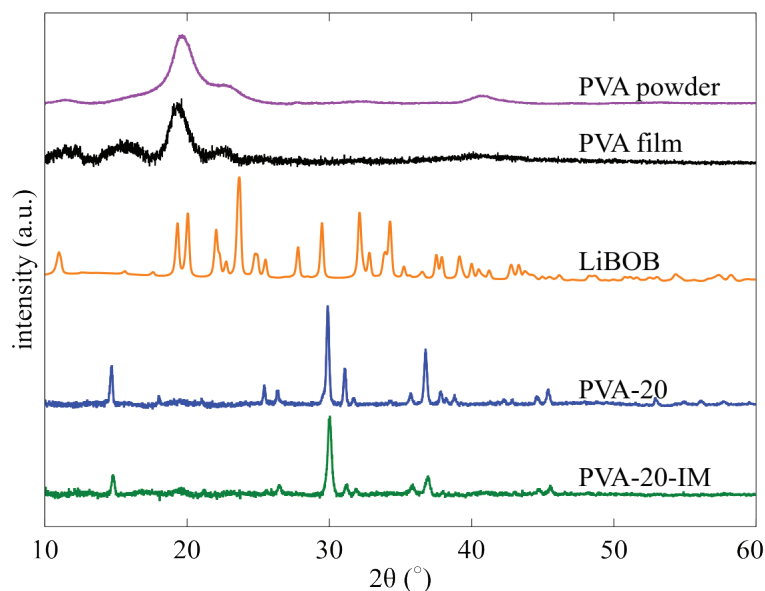


Figure 4: XRD spectra of PVA powder, PVA-0, LiBOB, PVA-20 and PVA-20-IM.

Addition of electrolyte salt is enough to disrupt the hydrogen bonding along the major chain, causing PVA to withstand dissolution in the salt solution during immersion.<sup>12</sup> It can be seen with decreasing crystallinity with the introduction of electrolyte salt, as presented on spectra PVA-20 as well as PVA-20-IM (4<sup>th</sup> and 5<sup>th</sup> from the top, respectively) on Figure 4.

Swelling behaviour during salt immersion can be observed on Figure 5. Increase in electrolyte uptake might still be possible even after 72 h but most likely become disadvantageous since deposits of crystal hydrates started to appear on the surface of the membrane, as seen on the inset picture. The appearance of these crystals was observed after 48 h of immersion, and the white spots continued to grow until last sampling measurement.

ICP measurement was taken on the salt solution right before (0 h) and after 72 h of immersion. The result shows that Li concentration in the solution has decreased from 41,088 ppm to 33,606 ppm which indicated 18.21% Li uptake on the membrane. This resulted in the upsurge of ionic conductivity of the CPE membrane, as discussed below in the EIS section.

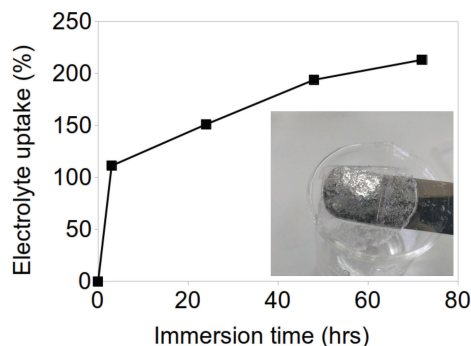


Figure 5: Electrolyte uptake curve of CPE membrane during salt immersion.

Nyquist plot from EIS measurement was presented on Figure 6. Typically, the plot involves a semicircle at high frequency range and a line at lower frequency, where they represent charge-transfer impedance (bulk material properties) and Li-ion diffusion impedance on the electrolyte/electrode interface, respectively.<sup>21</sup> solar cells, batteries and supercapacitors. Two types of polymers have been used; synthetic and natural polymers. This article discusses solid and gel polymer electrolytes (GPEs Bulk resistivity value acquired from the plot was then used to calculate membrane ionic conductivity,  $\eta$ , equation  $\eta = t/(Rb \cdot A)$  where  $t$  stands for polymer electrolyte thickness,  $A$  for electrode area, and  $Rb$  for bulk resistance obtained from the impedance plot, where the curve on high frequency area intercepts the real impedance axis. An equivalent circuit was obtained from curve fitting using EIS Spectra Analyser software, indicating bulk resistivity  $R$  as well as interfacial interaction indicating by constant phase element CPE and Warburg impedance  $W$ .<sup>22,23</sup>

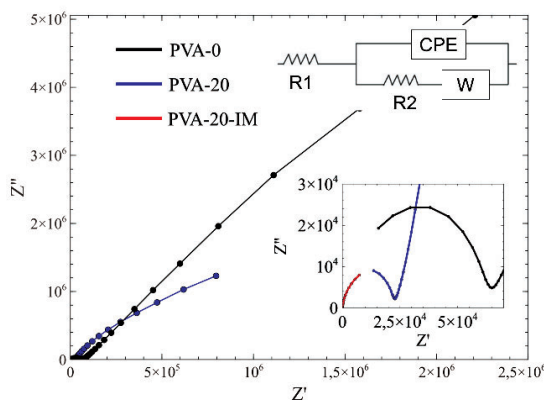


Figure 6: Nyquist plot of neat PVA membrane (PVA-0) as well as CPE membrane before (PVA-20) and after (PVA-20-IM) immersion process.



Ionic conductivities of the samples are summarised in Table 1. Addition of salt electrolyte in sample PVA-20 resulted in less than  $0.1 \mu\text{S/cm}$  increase in the ionic conductivity;  $4.77 \times 10^{-7} \text{ S/cm}$  is far too low to substitute liquid electrolyte. This could be attributed to limited amount of Li-ion as charge carrier.

Table 1: Ionic conductivity of CPE membranes.

Sample	Ionic Conductivity (S/cm)
PVA-0	$3.95 \times 10^{-7}$
PVA-20	$4.77 \times 10^{-7}$
PVA-20-IM	$2.06 \times 10^{-3}$

Hydrophilicity of PVA and LiBOB salt would aid the attempt to increase the salt concentration to enhance the ionic conductivity, provided minimum salt aggregation and maximum salt dissociation.<sup>24,25</sup> Careful consideration of salt addition has been described by Wang et al. who observed decreasing ionic conductivity with increasing salt concentration.<sup>26</sup> It should also be noted, however, that lithium salt anion has a great influence to stable SEI film formation as well as solvation-desolvation process.<sup>27</sup>

#### 4. CONCLUSION

Composite polymer electrolyte with PVA as polymer host and LiBOB salt as electrolyte has been fabricated through solution cast technique, producing free-standing membrane. Deionised water was capable to dissolve both PVA and LiBOB salt into homogeneous slurry, indicating that this process is potentially scalable in the future. FTIR result has shown slight amount of adsorbed moisture, but no decomposition products were found, suggesting this CPE is stable in room temperature. Immersion of CPE in LiBOB solution in water presented significant increase in ionic conductivity, from  $4.77 \times 10^{-7} \text{ S/cm}$  to  $2.06 \times 10^{-3} \text{ S/cm}$ , as calculated using impedance data obtained from EIS measurement. Li uptake during immersion was found to be 18.21% at equilibrium. Considering recent breakthrough on solid-state batteries for electric vehicles, this PVA-LiBOB-based CPE is highly viable as it employs more environmentally friendly materials compared to conventional Li-ion battery with carbonate-based liquid electrolyte.

## 5. ACKNOWLEDGEMENTS

The authors would like to express our gratitude to the Research Center for Advanced Materials and the Integrated Laboratory of the National Research and Innovation Agency (Badan Riset dan Inovasi Nasional, BRIN) for supporting the laboratory work and material characterisations. This work was financially supported by the 2<sup>nd</sup> Batch of National Priority Research Program from the Deputy of Engineering Sciences, Indonesian Institute of Sciences (LIPI) No. 58/A/DT/2021.

## 6. REFERENCES

1. Yang, P. et al. (2014). Gel polymer electrolyte based on polyvinylidene fluoride-co-hexafluoropropylene and ionic liquid for lithium ion battery. *Electrochim. Acta.*, 115, 454–460. <https://doi.org/10.1016/j.electacta.2013.10.202>
2. Nunes-Pereira, J. et al. (2015). Polymer composites and blends for battery separators: State of the art, challenges and future trends. *J. Power Sources*, 281, 378–398. <https://doi.org/10.1016/j.jpowsour.2015.02.010>
3. Zhou, D. et al. (2019). Polymer electrolytes for lithium-based batteries: Advances and prospects. *Chem.*, 5(9), 2326–2352. <https://doi.org/10.1016/j.chempr.2019.05.009>
4. Cui, Y. et al. (2020). A fireproof, lightweight, polymer-polymer solid-state electrolyte for safe lithium batteries. *Nano Lett.*, 20(3), 1686–1692. <https://doi.org/10.1021/acs.nanolett.9b04815>
5. Agrawal, R. C. & Pandey, G. P. (2008). Solid polymer electrolytes: Materials designing and all-solid-state battery applications: An overview. *J. Phys. D. Appl. Phys.*, 41, 223001. <https://doi.org/10.1088/0022-3727/41/22/223001>
6. Long, L. et al. (2016). Polymer electrolytes for lithium polymer batteries. *J. Mater. Chem. A*, 4, 10038–10039. <https://doi.org/10.1039/c6ta02621d>
7. Johan, M. R. et al. (2011). Effects of Al<sub>2</sub>O<sub>3</sub> nanofiller and EC plasticizer on the ionic conductivity enhancement of solid PEO–LiCF<sub>3</sub>SO<sub>3</sub> solid polymer electrolyte. *Solid State Ionics*, 196(1), 41–47. <https://doi.org/10.1016/j.ssi.2011.06.001>
8. Zinigrad, E. et al. (2007). On the thermal behavior of Li bis(oxalato)borate LiBOB. *Thermochim. Acta*, 457(1–2), 64–69. <https://doi.org/10.1016/j.tca.2007.03.001>
9. Li, C. et al. (2019). Studies of air-exposure effects and remediation measures on lithium bis(oxalato)borate. *New J. Chem.*, 43(36), 14238–14245. <https://doi.org/10.1039/c9nj03468d>
10. Sumathipala, H. H. et al. (2007). High performance PEO-based polymer electrolytes and their application in rechargeable lithium polymer batteries. *Ionics (Kiel)*, 13, 281–286. <https://doi.org/10.1007/s11581-007-0137-4>
11. Hirankumar, G. & Mehta, N. (2018). Effect of incorporation of different plasticizers on structural and ion transport properties of PVA–LiClO<sub>4</sub> based electrolytes. *Heliyon*, 4(12), e00992. <https://doi.org/10.1016/j.heliyon.2018.e00992>

12. Hassan, C. M. et al. (2005). Water Solubility Characteristics of Poly(vinyl alcohol) and Gels Prepared by Freezing/Thawing Processes. *Water Soluble Polym.*, 31–40. [https://doi.org/10.1007/0-306-46915-4\\_3](https://doi.org/10.1007/0-306-46915-4_3)
13. Lv, P. et al. (2018). Robust succinonitrile-based gel polymer electrolyte for lithium-ion batteries withstanding mechanical folding and high temperature. *ACS Appl. Mater. Interfaces.*, 10(30), 25384–25392. <https://doi.org/10.1021/acsami.8b06800>
14. Ma, T. et al. (2013). Preparation of PVDF based blend microporous membranes for lithium ion batteries by thermally induced phase separation : I . Effect of PMMA on the membrane formation process and the properties. *J. Memb. Sci.*, 444, 213–222. <https://doi.org/10.1016/j.memsci.2013.05.028>
15. Yang, L. et al. (2020). Study on boron-containing electrolytes at extra-high temperatures for lithium-ion batteries. *Sustain. Energy Fuels*, 4(8), 4126–4136. <https://doi.org/10.1039/d0se00529k>
16. Zhang, Z. et al. (2015). Radiation-crosslinked nanofiber membranes with well-designed core–shell structure for high performance of gel polymer electrolytes. *J. Memb. Sci.* 492, 77–87. <https://doi.org/10.1016/j.memsci.2015.05.040>
17. Zhu, Y. S. et al. (2013). A new single-ion polymer electrolyte based on polyvinyl alcohol for lithium ion batteries. *Electrochim. Acta*, 87, 113–118. <https://doi.org/10.1016/j.electacta.2012.08.114>
18. Premila, R. et al. (2018). Experimental investigation of nano filler TiO<sub>2</sub> doped composite polymer electrolytes for lithium ion batteries. *Appl. Surf. Sci.*, 449, 426–434. <https://doi.org/10.1016/j.apsusc.2017.11.272>
19. Wigayati, E. M. et al. (2016). Synthesis and characterization of LiBOB as electrolyte for lithium-ion battery. *Ionics (Kiel)*, 22, 43–50. <https://doi.org/10.1007/s11581-015-1531-y>
20. Rajendran, S. et al. (2004). Characterization of PVA-PVdF based solid polymer blend electrolytes. *Phys. B Condens. Matter.*, 348(1–4), 73–78. <https://doi.org/10.1016/j.physb.2003.11.073>
21. Yusuf, S. N. F. et al. (2019). Preparation and electrical characterization of polymer electrolytes: A review. *Mater. Today Proc.*, 17(2), 446–458. <https://doi.org/10.1016/j.matpr.2019.06.475>
22. Bondarenko, A. S. & Ragoisha, G. A. (2005). In Pomerantsev A. L. (Ed.). *Progress in Chemometrics Research*. New York: Nova Science Publishers, 89–102.
23. Vadhva, P. et al. (2021). Electrochemical Impedance Spectroscopy for All-Solid-State Batteries: Theory, Methods and Future Outlook. *ChemElectroChem* 8, 1930–1947. <https://doi.org/10.1016/j.jpowsour.2018.10.045>
24. Li, Y. et al. (2018). Ambient temperature solid-state Li-battery based on high-salt-concentrated solid polymeric electrolyte. *J. Power Sources*, 397, 95–101. <https://doi.org/10.1016/j.jpowsour.2018.05.050>
25. Zhao, Y. et al. (2018). A rational design of solid polymer electrolyte with high salt concentration for lithium battery. *J. Power Sources*, 407, 23–30. <https://doi.org/10.1016/j.jpowsour.2018.10.045>

26. Wang, J. et al. (2021). Analyzing the mechanism of functional groups in phosphate additives on the interface of  $\text{LiNi}_{0.8}\text{Co}_{0.15}\text{Al}_{0.05}\text{O}_2$  cathode materials. *ACS Appl. Mater. Interfaces*, 13(14), 16939–16951. <https://doi.org/10.1021/acsami.0c21535>
27. Li, S. Y. et al. (2022). Anions tuned solid electrolyte interphase in lithium-ion batteries. *Batter. Supercaps*, 5(2), 1–8. <https://doi.org/10.1002/batt.202100274>